THE EUROPEAN
PHYSICAL JOURNAL C

Search for nucleon decays induced by GUT magnetic monopoles with the MACRO experiment

M. Ambrosio[12], R. Antolini[7], G. Auriemma[14,a], D. Bakari[2,17], A. Baldini[13], G. C. Barbarino[12], B. C. Barish[4], G. Battistoni[6,b], Y. Becherini[2], R. Bellotti[1], C. Bemporad[13], P. Bernardini[10], H. Bilokon[6], C. Bloise[6], C. Bower[8], M. Brigida[1], S. Bussino[18], F. Cafagna[1], M. Calicchio[1], D. Campana[12], M. Carboni[6], R. Caruso[9], S. Cecchini[2,c], F. Cei[13], V. Chiarella[6], B. C. Choudhary[4], S. Coutu[11,i], M. Cozzi[2], G. De Cataldo[1], H. Dekhissi[2,17], C. De Marzo[1], I. De Mitri[10], J. Derkaoui[2,17], M. De Vincenzi[18], A. Di Credico[7], O. Erriquez[1], C. Favuzzi[1], C. Forti[6], P. Fusco[1], G. Giacomelli[2], G. Giannini[13,d], N. Giglietto[1], M. Giorgini[2], M. Grassi[13], A. Grillo[7], F. Guarino[12], C. Gustavino[7], A. Habig[3,p], K. Hanson[11], R. Heinz[8], E. Iarocci[6,e], E. Katsavounidis[4,q], I. Katsavounidis[4,r], E. Kearns[3], H. Kim[4], S. Kyriazopoulou[4], E. Lamanna[14,l], C. Lane[5], D. S. Levin[11], P. Lipari[14], N. P. Longley[4,h], M. J. Longo[11], F. Loparco[1], F. Maaroufi[2,17], G. Mancarella[10], G. Mandrioli[2], S. Manzoor[2,n], A. Margiotta[2], A. Marini[6], D. Martello[10], A. Marzari-Chiesa[16], M. N. Mazziotta[1], D. G. Michael[4], P. Monacelli[9], T. Montaruli[1], M. Monteno[16], S. Mufson[8], J. Musser[8], D. Nicolò[13], R. Nolty[4], C. Orth[3], G. Osteria[12], O. Palamara[7], V. Patera[6,e], L. Patrizii[2], R. Pazzi[13], C. W. Peck[4], L. Perrone[10], S. Petrera[9], P. Pistilli[18], V. Popa[2,g], A. Rainò[1], J. Reynoldson[7], F. Ronga[6], A. Rrhioua[2,17], C. Satriano[14,a], E. Scapparone[7], K. Scholberg[3,q], A. Sciubba[6,e], P. Serra[2], M. Sioli[2], G. Sirri[2], M. Sitta[16,o,*], P. Spinelli[1], M. Spinetti[6], M. Spurio[2], R. Steinberg[5], J. L. Stone[3], L. R. Sulak[3], A. Surdo[10], G. Tarlè[11], V. Togo[2], M. Vakili[15,s], C. W. Walter[3], R. Webb[15]

[1] Dipartimento di Fisica dell'Università di Bari and INFN, 70126 Bari, Italy
[2] Dipartimento di Fisica dell'Università di Bologna and INFN, 40126 Bologna, Italy
[3] Physics Department, Boston University, Boston, MA 02215, USA
[4] California Institute of Technology, Pasadena, CA 91125, USA
[5] Department of Physics, Drexel University, Philadelphia, PA 19104, USA
[6] Laboratori Nazionali di Frascati dell'INFN, 00044 Frascati (Roma), Italy
[7] Laboratori Nazionali del Gran Sasso dell'INFN, 67010 Assergi (L'Aquila), Italy
[8] Depts. of Physics and of Astronomy, Indiana University, Bloomington, IN 47405, USA
[9] Dipartimento di Fisica dell'Università dell'Aquila and INFN, 67100 L'Aquila, Italy
[10] Dipartimento di Fisica dell'Università di Lecce and INFN, 73100 Lecce, Italy
[11] Department of Physics, University of Michigan, Ann Arbor, MI 48109, USA
[12] Dipartimento di Fisica dell'Università di Napoli and INFN, 80125 Napoli, Italy
[13] Dipartimento di Fisica dell'Università di Pisa and INFN, 56010 Pisa, Italy
[14] Dipartimento di Fisica dell'Università di Roma "La Sapienza" and INFN, 00185 Roma, Italy
[15] Physics Department, Texas A&M University, College Station, TX 77843, USA
[16] Dipartimento di Fisica Sperimentale dell'Università di Torino and INFN, 10125 Torino, Italy
[17] L.P.T.P, Faculty of Sciences, University Mohamed I, B.P. 524 Oujda, Morocco
[18] Dipartimento di Fisica dell'Università di Roma Tre and INFN Sezione Roma Tre, 00146 Roma, Italy

Abstract. The interaction of a Grand Unification Magnetic Monopole with a nucleon can lead to a barion–number violating process in which the nucleon decays into a lepton and one or more mesons (catalysis of nucleon decay). In this paper we report an experimental study of the effects of a catalysis process in the MACRO detector. Using a dedicated analysis we obtain new magnetic monopole (MM) flux upper limits at the level of $\sim 3 \cdot 10^{-16}\ cm^{-2}\ s^{-1}\ sr^{-1}$ for $1.1 \cdot 10^{-4} \leq |\beta| \leq 5 \cdot 10^{-3}$, based on the search for catalysis events in the MACRO data. We also analyze the dependence of the MM flux limit on the catalysis cross section.

[a] Also Università della Basilicata, 85100 Potenza, Italy
[b] Also INFN Milano, 20133 Milano, Italy
[c] Also Istituto IASF/CNR, 40129 Bologna, Italy
[d] Also Università di Trieste and INFN, 34100 Trieste, Italy
[e] Also Dipartimento di Energetica, Università di Roma, 00185 Roma, Italy
[g] Also Institute for Space Sciences, 76900 Bucharest, Romania

[h] Macalester College, Dept. of Physics and Astr., St. Paul, MN 55105
[i] Also Department of Physics, Pennsylvania State University, University Park, PA 16801, USA
[l] Also Dipartimento di Fisica dell'Università della Calabria, Rende (Cosenza), Italy
[n] Also RPD, PINSTECH, P.O. Nilore, Islamabad, Pakistan

1 Introduction

The supermassive magnetic monopoles (MMs) predicted by the Grand Unified Theories of the electroweak and strong interactions (GUTs) have a core in which the original Grand Unification symmetry is restored [1]. The interaction of a nucleon with the MM core can lead to a reaction in which the nucleon decays (catalysis of nucleon decay). The cross section for this process is of the order of the geometrical cross section of the MM core, $\sigma \sim 10^{-56} \ cm^2$ [2,3], practically negligible. In 1982 Rubakov [4,5] and Callan [6,7] were independently led to the conclusion that this catalysis process may proceed via another mechanism and have a much higher cross section, of the same order of magnitude of the strong interaction cross sections.

The Rubakov–Callan mechanism is completely different from the spontaneous decay and so are the corresponding final states. The main decay channels are $e^+\pi^0$ and μ^+K^0 for the proton decay and $e^+\pi^-$ and μ^+K^- for the neutron decay. According to the theoretical calculations, pions should always come with positrons, strange particles with muons, and there should be no neutrinos in the final states [3].

The catalysis cross section takes the form [3,7,8]

$$\sigma_{\Delta B \neq 0} = \frac{\sigma_0}{\beta} \qquad (1)$$

where β is the MM velocity and σ_0 is a parameter, of the order of the cross sections of the strong interactions, which depends on the explicit QCD calculations. According to some authors [5,9] however the cross section for proton decay has the form $\sigma \propto 1/\beta^2$, so a $1/\beta$ enhancement factor is expected in this case. In addition there could be suppression factors for protons in a nucleus [9].

In the hypothesis of a non negligible cross section, the MM induced nucleon decay can be exploited to detect the passage of a MM in an apparatus. Many proton decay experiments (like Soudan [10], IMB [11] and Kamiokande [12]) and neutrino telescopes (such as the Lake Baikal detector [13]) have searched for monopoles via the catalysis mechanism: a MM could have been identified as a series of decay events more or less along a straight line. All these experiments have established limits to the MM flux.

Beside these direct searches, bounds to the local monopole flux can be set by means of the catalysis process in an indirect way. Astrophysical objects such as neutron stars, white dwarfs and also planets can accumulate MMs by capturing the ones that impinge upon them [2]. In the presence of nuclear matter a MM is able to release energy via the nucleon decay catalysis. The limits are established by requiring the the energy released by the catalysis cannot be greater than the observed one: in this way it is

possible to set an upper limit to the number of contained MMs and then to translate it into a bound to the local MM flux [2,14,15].

MACRO was a large scale multi–purpose detector located in the Gran Sasso underground laboratory, optimized in the search for GUT magnetic monopoles with velocity $\beta \geq 4 \cdot 10^{-5}$ and with a sensitivity well below the Parker bound as defined in [16]. Direct searches for MMs were made using various subdetectors both in a stand-alone and in a combined way in different ranges of velocity. The final results on the upper limits to the MM flux are given in [17]; previous results can be found also in [18–22]. These limits refer to a direct detection of bare magnetic monopoles of one unit Dirac charge ($g_D = 137/2e$), catalysis cross section $\sigma_{cat} < 1 \ mb$ and isotropic flux.

In this paper we present a different approach to the search for magnetic monopoles using the nucleon decay process. We developed a dedicated analysis procedure aiming to detect nucleon decay events induced by the passage of a GUT MM in the MACRO detector; the results of this search are reported as a function of the MM velocity and the catalysis cross section. After summarizing the properties of the MACRO streamer tube subsystem (Sect. 2), the subdetector used in the present analysis, we describe the simulation technique employed to study the characteristics of a catalysis process in the detector (Sect. 3). The analysis criteria used in the search for these particular events in the streamer tube data are reported in Sect. 4, and the results of the real MACRO data analysis in Sect. 5. The previously published MACRO MM search with the horizontal streamer tube subsystem is based on a different analysis pattern in which the catalysis process is considered negligible; in Sect. 6 we discuss how this analysis may be affected by the induced nucleon decay and how the obtained upper limits to the MM flux depend on the catalysis cross sections. The conclusions are given in Sect. 7.

2 The MACRO detector

MACRO had total dimensions of $76.5 \times 12 \times 9.3 \ m^3$, and consisted of six "supermodules" arranged in a modular structure; each supermodule was divided into a lower and an upper part, both equipped with streamer tubes and liquid scintillation counters; in addition one horizontal and two vertical planes of nuclear track detector were also present. A detailed description of the apparatus can be found in [23,24]. Special care was taken to ensure that the three types of detectors and the readout electronics were sensitive to low β particles. A single candidate event could have provided distinctive and multiple signatures in the three subdetectors, so the experiment had enough redundancy of information to attain unequivocal and reliable interpretation on the basis of only few or even one event.

We looked for catalysis events in the data collected with the streamer tube subsystem. Among the MACRO subdetectors the streamer tubes could be the most sensitive to the catalysis process, having a sufficient combination of spatial and temporal resolution to clearly sep-

[o] Also Dipartimento di Scienze e Tecnologie Avanzate, Università del Piemonte Orientale, Alessandria, Italy
[p] Also U. Minn. Duluth Physics Dept., Duluth, MN 55812
[q] Also Dept. of Physics, MIT, Cambridge, MA 02139
[r] Also Intervideo Inc., Torrance CA 90505 USA
[s] Also Resonance Photonics, Markham, Ontario, Canada
[*] *Corresponding author*: sitta@to.infn.it

arate the MM track from the catalysis products. For the same reasons the streamer tube standard analyses could be heavily affected by a possible catalysis event, therefore we studied as well how the corresponding flux upper limit varies with the catalysis cross section. Below we give more details on the streamer tube subsystem.

The lower part of a MACRO supermodule was equipped with two horizontal planes of scintillation counters and ten horizontal planes of streamer tubes interleaved with seven rock absorber layers; the upper part was equipped with one horizontal plane of scintillation counters and four horizontal planes of streamer tubes without any absorber. The vertical west and east walls of the apparatus were covered with six planes of vertical streamer tubes interleaved with one vertical plane of scintillation counters; the frontal walls of the lower part were covered with a similar structure. The tubes were filled with a Helium–n-pentane mixture, in order to exploit the Drell–Penning effect [25,26] in detecting MMs, and operated in the limited streamer mode. The cell dimensions and the charge drift in the gas produced a time jitter, which resulted in a time resolution of about 140 ns.

The streamer tube electronics were designed to be effective in the search for slow charged particles with $\beta = v/c$ down to 10^{-4}. Both the analog and digital part of the tube signal were recorded. The analog part was used to measure the time and charge of the streamer hits by means of a dedicated circuit, the QTP system [23,24], with a time resolution of 150 ns and a charge resolution of $\sim 5\%$ the typical charge released by a minimum ionizing particle. Charge and time information was kept in a cyclic 640 μs deep memory. The digital part was used to determine the spatial coordinate along a direction perpendicular to the tube anode wires, with a resolution of about 1.1 cm; stereo pick-up strips were used to determine a second independent spatial coordinate with a resolution of about 1.2 cm. Combining these informations it is possible to reconstruct the particle track in two space views and in a time view.

Two independent MM triggers employing the streamer tube signals were implemented, one with the horizontal planes of the lower part and one with the vertical planes. The only assumption made in designing the triggers was that a heavy slow-moving particle can cross the detector without any apparent variation of direction or speed (which is the case of GUT MMs). In this work only the trigger on the horizontal planes was used. The primary function of this trigger was to measure the time-of-flight of particles in the range $3 \cdot 10^{-5} \leq \beta \leq 1$ and distinguish them from random noise. The digital OR of all wires belonging to one plane was summed to the corresponding signals from the next module, and then fed to the trigger circuitry, which acted as 320 delayed coincidences (called β-slices) representing the time-of-flight from plane 10 to plane 1 with a resolution of 3 μs. The trigger fired when the signals from at least seven planes of two consecutive modules were aligned in time.

A complete description of the streamer tube hardware and the corresponding triggers can be found in [19,23,24, 27].

3 The simulation

To study the expected characteristics of the catalysis events induced in MACRO and their consequences on the data analysis and results, a detailed MonteCarlo simulation of the physical process in the detector was performed.

The simulation of the catalysis process was independent of MACRO (and actually can be applied to any detector set-up). The total cross section for the catalysis was left as a free parameter of the simulation; the decay channels and the branching ratios were chosen according to [3, 8], namely $n, p \rightarrow e^+\pi$ and $n, p \rightarrow \mu^+ K$ with branching ratios 90% and 10%, respectively.

Several improvements to GMACRO, the GEANT-based simulation code of the detector, were introduced. They concern a detailed description of the streamer acquisition electronics, which took into account the hit time correlation when multiple charges on wires and strips were recorded, the dead time of the streamer acquisition chain, and the charge and time digitization performed by the QTP system. It was inserted as well the simulation of the streamer tube MM trigger on the horizontal wire planes, with a description of its response to particles of different velocities and of its interaction with the streamer data acquisition. In all these tasks we reproduced the behaviour of the real electronic components.

Many samples of simulated events with different (and constant) MM velocities and catalysis cross sections were simulated. Each sample consisted of 10,000 single MM tracks generated from an isotropic flux. Five cross section values were used, namely $\sigma_{cat} = 0, 10^{-26}, 10^{-25}, 5 \cdot 10^{-25}$ and 10^{-24} cm^2 ($\sigma_{cat} = 0$ means no catalysis and is used as a reference). For each cross section 5 (7 for $5 \cdot 10^{-25}$ and 10^{-24} cm^2) MM velocities were simulated: $\beta = 10^{-2}, 5 \cdot 10^{-3}, 10^{-3}, 5 \cdot 10^{-4}$ and 10^{-4} (plus $2 \cdot 10^{-3}$ and $2 \cdot 10^{-4}$ for the larger σ). We kept constant the cross section on nucleon σ and not the parameter σ_0 (see (1)), due to the uncertainties on both the β dependence and the possible suppression factors on various nuclei. In this way our results are independent of the theoretical models, and can be used directly to place limits on the cross section parameters.

We did not include in our simulation the rock around the detector, unlike other experiments which took into account the possibility of a premature trigger due to a catalysis event in the surrounding rock. In fact, given its trigger logic, the streamer tube MM trigger on the horizontal planes could not be activated by the decay products coming from a catalysis event in the external rock. However in case of a fast particle trigger, the trigger signal was conveniently delayed to let any slow moving particle cross and leave the detector, which was not put immediately in dead time [27]. Therefore we considered only MM catalysed nucleon decays inside the detector.

As mentioned in the Introduction, for the cross section of the induced proton decay there are two theoretical models: it could be either proportional to $1/\beta$ as the cross section of the neutron decay, or to $1/\beta^2$. In the latter case the proton cross section is enhanced by a factor $1/\beta$ with respect to the neutron decay. To take into account both
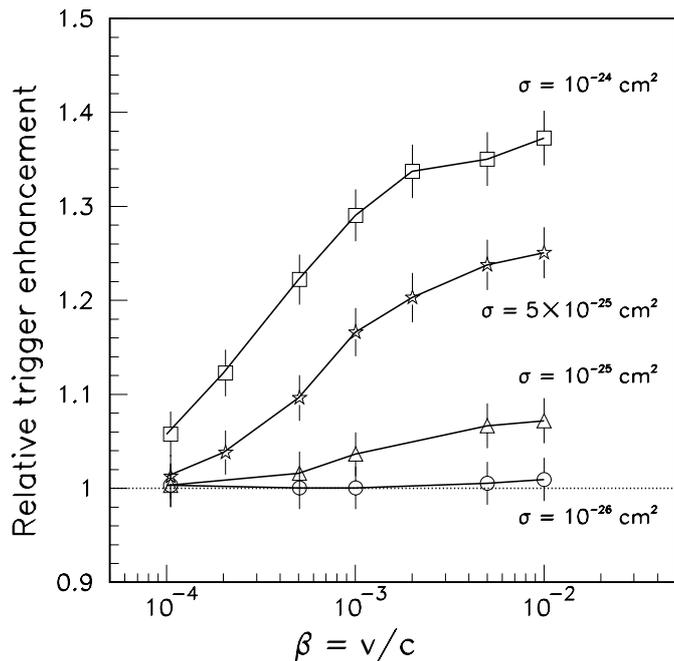
Fig. 1. Ratio of the total number of streamer MM triggers in a given sample to the total number of streamer MM triggers in the sample without catalysis

Fig. 2. Ratio of the number of selected events in a given sample to the number of selected events in the sample without catalysis

models, for each value of the total cross section σ_{cat} and for each β we performed two simulations: in one of them the decay probabilities of a proton and of a neutron were equal, in the other one the probability of a proton decay was enhanced by a factor $1/\beta$ with respect to the probability of a neutron decay. The results showed a very small difference in the MACRO response to the two models, well inside the statistical errors. In the following we show the results only for the model in which both cross sections are equal, the results for the other model being very similar; when physical conclusions are drawn, results for both of them are given.

From the experimental point of view it is interesting to notice how the detector response changes due to the catalysis process. Figure 1 shows the ratio of the total number of streamer MM triggers in a given sample over the number of streamer triggers in the sample without catalysis (i.e. with $\sigma_{cat} = 0$) for the same β (in this Figure and in all the subsequent ones the error bars are statistical, and smaller than the marker size where they do not appear; only the samples at the marker position were simulated and analyzed, the connecting lines serve only as a guide to the eye). Clearly the number of triggers increases with σ_{cat} and the MM β, since the wire signals produced by the decay products can contribute to the trigger formation. There can be even $\sim 40\%$ more triggers for the highest values of σ_{cat} and β which were simulated. The trigger increase is small at low velocities and larger at high velocities, because the catalysis hits are very near to each other in time and can easily contribute to activate the lower trigger β-slices (the ones triggered by fast moving particles), but can rarely contribute to the higher ones (interested by slow moving particles). For $\sigma = 10^{-24}\ cm^2$ there are
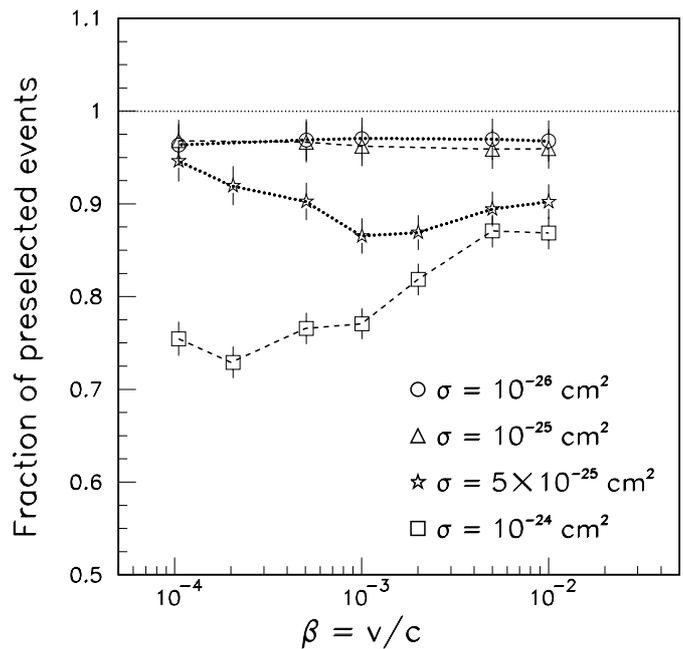
so many catalyses per event that the secondary particles hits can activate the trigger by themselves, determining the larger value of the trigger ratio also for the lowest β value.

4 Search for nucleon decay events

All the MonteCarlo samples were analyzed with exactly the same programs used later on for the real data. Only the horizontal streamer planes of the lower MACRO participated to the trigger formation, but for the event reconstruction all horizontal planes belonging to both the lower and the upper parts of the detector were used.

Events were preselected by requiring

1. at least one space track matching in both space views
2. each track must have at least 5 points in each view
3. in case of multiple wire tracks, at least one "non–parallel" track
4. at least one time track with $|ToF| \geq 0.8\ \mu s$

Conditions 1 and 2 identify good MM tracks, the third one rejects multiple muons from cosmic rays, which sometimes may confuse the time tracking. The last condition selects slow moving particles (a time-of-flight of 0.8 μs corresponds to a MM crossing vertically the ten lower horizontal planes with $\beta = 2 \cdot 10^{-2}$, a value well above the upper validity limit of the streamer tube analyses).

In Fig. 2 the ratio of the number of selected events in a given sample over the number of selected events in the sample without catalysis is shown as a function of the MM β and the catalysis cross section σ_{cat}; this ratio is actually the relative efficiency with respect to the case of no catalysis. The main reason of inefficiency is a wrong
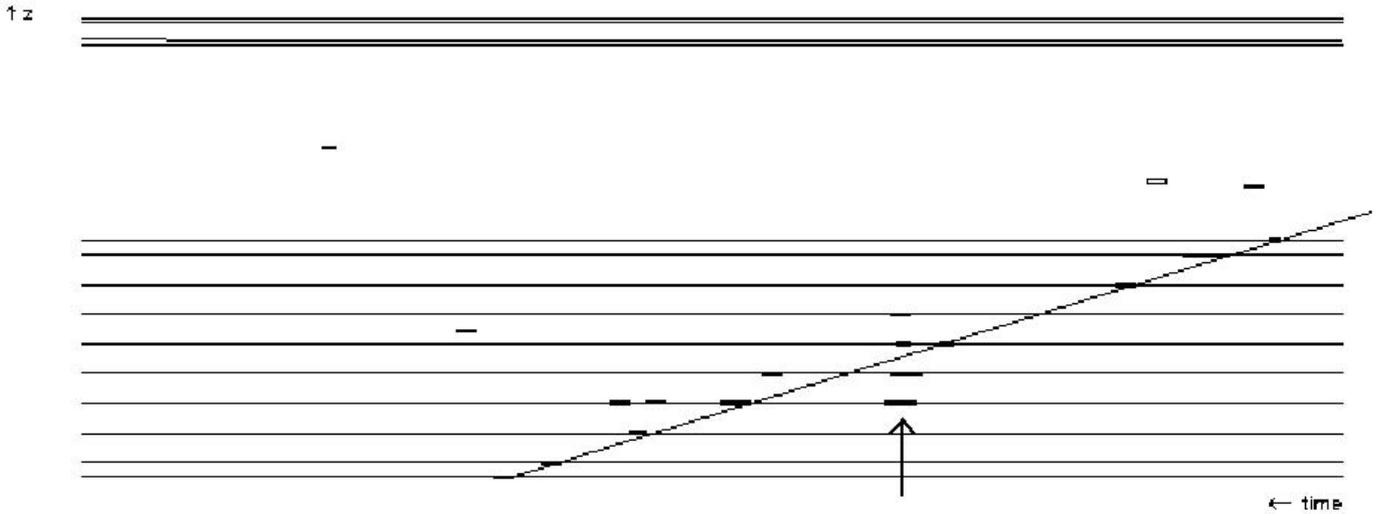
Fig. 3. Time view of a simulated MM induced nucleon decay inside the detector: the reconstructed slow MM track and the fast particles hits (at the arrow position) are clearly distinguishable

ToF estimation because sometimes when there are many catalysis hits the time fit may get confused and mix the MM signals with the secondary particle ones, giving thus a time-of-flight lower than the actual value. Clearly the cleaner the event the more correct the ToF computation, so for small cross sections this effect is negligible, while it is much more relevant for large cross sections. As a consequence these criteria result more efficient in selecting low σ_{cat} events, and even more efficient for no catalysis events. Nevertheless these cuts, the ToF cut in particular, cannot be relaxed without contaminating the preselected samples from real data with atmospheric muons events (especially if accompanied by noise or showers).

By examining the simulated events it appears that the space view of a catalyzed decay is indistinguishable from a cosmic muon accompanied by some noise, while it has a typical pattern in the time view: a slow track due to the MM with some "fast" hits, generated by the catalysis products, contained in a small ($\lesssim 1~\mu s$) time window. In Fig. 3 the time view of a simulated catalysis event is shown: the slow track of the MM crossing the detector and the hits of the fast decay particles (at the arrow position) are clearly distinguishable. This peculiar signature can be exploited in a catalysis–oriented analysis, which is applied to the events selected with the preliminary cuts described above. The characteristics of the time view of a catalysis event, and in particular the presence of fast hits grouped together along an almost vertical track, are the main feature used in the present search for catalyzed nucleon decays, while being a possible source of inefficiency for the previously published MACRO direct MM searches with the streamer tubes, which assumed no decay induced by the MM. Although the space view cannot be used to tag an event as a catalysis candidate, nevertheless some space consistency must be required anyway, for instance the catalysis hits cannot be too far from the MM track.

Since the streamer trigger requires at least 7 planes, a track must consist of at least 7 points. In the present anal-

ysis this condition had to be loosened, since also the catalysis hits can contribute to the trigger formation, which may be activated even by shorter tracks: so each track is required to consist of at least 5 points only. If the MM traversed the detector, it must be reconstructed also in the time view and be a slow particle, hence a β cut had to be imposed to the time track. There must be a consistency between the wire and time views: the same planes must be present in the wire as in the time fit, since they are both reconstructed from the signals coming from the same hardware elements; possible hardware inefficiencies are taken into account by leaving the possibility of 1 or 2 planes present in one fit and not in the other. Catalysis hits are searched for in $\pm 10~\mu s$ around the time track, because they cannot be too far in time from the MM. At least one catalysis hit must be within $1~m$ around a wire track: the catalysis must have been initiated in the vicinity of the MM; in this way we exclude random noise hits uncorrelated in space but accidentally near in time. All catalysis hits must be inside a $1~\mu s$ time window, since the decay products are fast particles. Finally, catalysis hits must be present on at least 3 out of 4 consecutive planes: this is the minimum requirement needed to clearly identify a catalysis candidate while rejecting the background.

The above features have been implemented in the analysis of the preselected events following these steps:

1. select an event with at least one track in both the spatial and temporal views with at least 5 points
2. require no more than 2 planes fitted in either view and missing in the other one
3. for each time track with $|\beta| \leq 10^{-2}$, which is assumed to be the MM track, define a time window equal to the time intersection of the track with the first and tenth plane $\pm 10~\mu s$ in which to search for catalysis hits
4. if hits on at least 3 out of 4 consecutive planes in a $1~\mu s$ window are found, of which at least one within $1~m$ from any wire track and the other ones in $\pm 2~m$ from the first one, keep the event as a catalysis candidate.

Fig. 4. Fraction of preselected simulated events with catalysis which pass the catalysis specific cuts

Table 1. Results of the real data analysis

Cuts applied	Events survived
Total number of preselected events	86339
≤ 4 adjacent fired QTP channels	67565
Consistency of wire and time tracks	62130
Catalysis specific cuts	15
validity range: $1.1 \cdot 10^{-4} \leq |\beta| \leq 5 \cdot 10^{-3}$	0

were collected from January 1992 to September 2000, for a live time of 71193 hours; the full configuration detector acceptance, computed by means of a MonteCarlo simulation including geometrical and trigger requirements, was 4250 $m^2\ sr$.

From a visual scan of a small subsample of preselected real events, some of them were found to have heavy electronic noise: typically there are two or more horizontal planes in which all the QTP channels have fired; for this reason the corresponding time hits are biased, so as to compromise the ToF measurement. These events represent a clearly spurious background which the real samples are rich of. In order to reject the noisy events, a further cut was imposed on the preselected events before applying the catalysis identification analysis, namely to have no more than 4 adjacent fired QTP channels. This additional requirement had no effect on the simulated samples with lower cross sections, and was at the level of few percent for higher cross sections. The effect of this cut is already included in Fig. 5.

The events were preselected with the loose criteria described in the beginning of the Sect. 4; to these events the catalysis-specific cuts were applied. In Table 1 the number of events which remain after each cut is reported. No candidate survived, therefore upper limits to the monopole flux were set as a function of the cross section. We limited this analysis to the larger values since for $\sigma_{cat} \leq 10^{-25}$ cm^2 the global efficiency is too low. The time-integrated acceptance was the same as for the "standard" streamer tube analysis [17,19], since exactly the same real data sample was analyzed. The new upper limits are plotted as a function of β in Fig. 6: the solid lines represent the standard streamer limit in the hypothesis of no catalysis. Only the plotted points were actually computed, and the lines are only rough interpolations to guide the eye. The lowest bounds at $\beta = 10^{-4}$ are 2.99 and $3.38 \cdot 10^{-16}$ $cm^{-2}\ s^{-1}\ sr^{-1}$ for $\sigma_{cat} = 5 \cdot 10^{-25}$ cm^2 and 10^{-24} cm^2 respectively, for the model with equal cross sections, and 2.86 and $3.36 \cdot 10^{-16}$ $cm^{-2}\ s^{-1}\ sr^{-1}$ for the same cross section values, for the model which assumes a proton cross section enhancement by a factor $1/\beta$.

Figure 7 shows how the upper limit to the MM flux obtained with this new catalysis-oriented analysis varies as a function of the catalysis cross section σ_{cat} for two MM velocities $\beta = 10^{-4}$ and $\beta = 10^{-3}$.

Figure 4 shows the fraction of preselected simulated events with catalysis which meet all the aforementioned conditions. For the samples at low cross sections ($\sigma_{cat} \lesssim 10^{-25}$ cm^2) this analysis is very inefficient, so our limits will be significant only for larger cross sections. The strong decrease of the efficiency for $\beta = 10^{-2}$ is due to the β cut on the time track.

The same analysis scheme was applied also to the simulated sample without catalysis. No event remained, so we can conclude that these cuts have a 100% efficiency in rejecting simulated events without catalysis. As a further check, all events without catalysis contained in the samples at lower cross sections were rejected.

We required that the present catalysis search was valid in the range $1.1 \cdot 10^{-4} \leq |\beta| \leq 5 \cdot 10^{-3}$, which is the same range of the streamer standard analysis: the lower limit is the minimum MM velocity required for the Drell–Penning effect to take place, the upper limit is required to fully reject the atmospheric muon contamination. In Fig. 5 the fraction of initial events (that is, events contained in the MonteCarlo generated samples) which survive to all cuts (including the cut to reject the electronic noise, described in the next paragraph) for both cross section models is shown. This fraction can be considered the total efficiency of the present data analysis (the efficiency of the hardware is assumed to be the same of the published MACRO streamer tube analysis [17,19]).

5 Data analysis

The same analysis cuts described in the previous paragraph were applied to the whole sample of real data collected with the streamer tube MM trigger on the horizontal planes, the same sample used also in [17]. These data

6 Discussion of the results

As it can be seen from Fig. 6, the MM flux upper limit is very good at lower β, and becomes worse as the MM
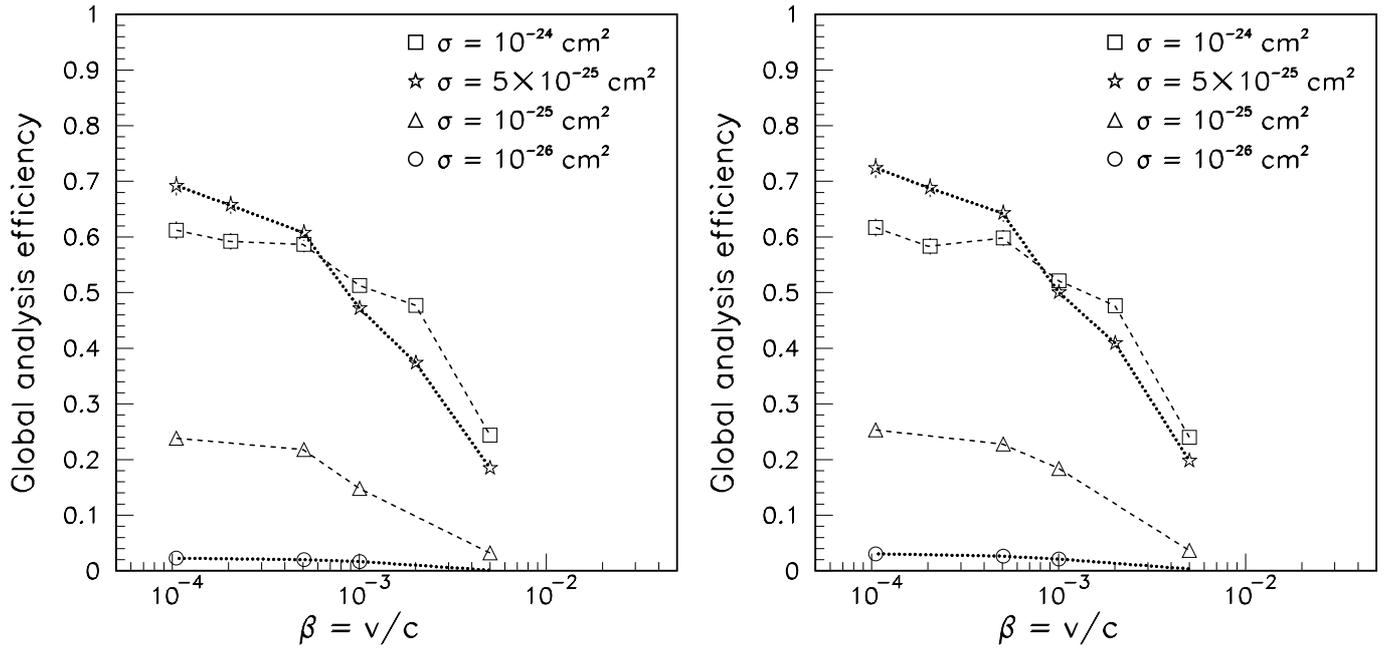
Fig. 5. Fraction of simulated events with catalysis identified by the analysis with respect to the total number of events in each sample as a function of the MM velocity for various cross section values (including the noise cut): equal cross sections for proton and neutron decay on the left, enhanced proton decay cross section on the right
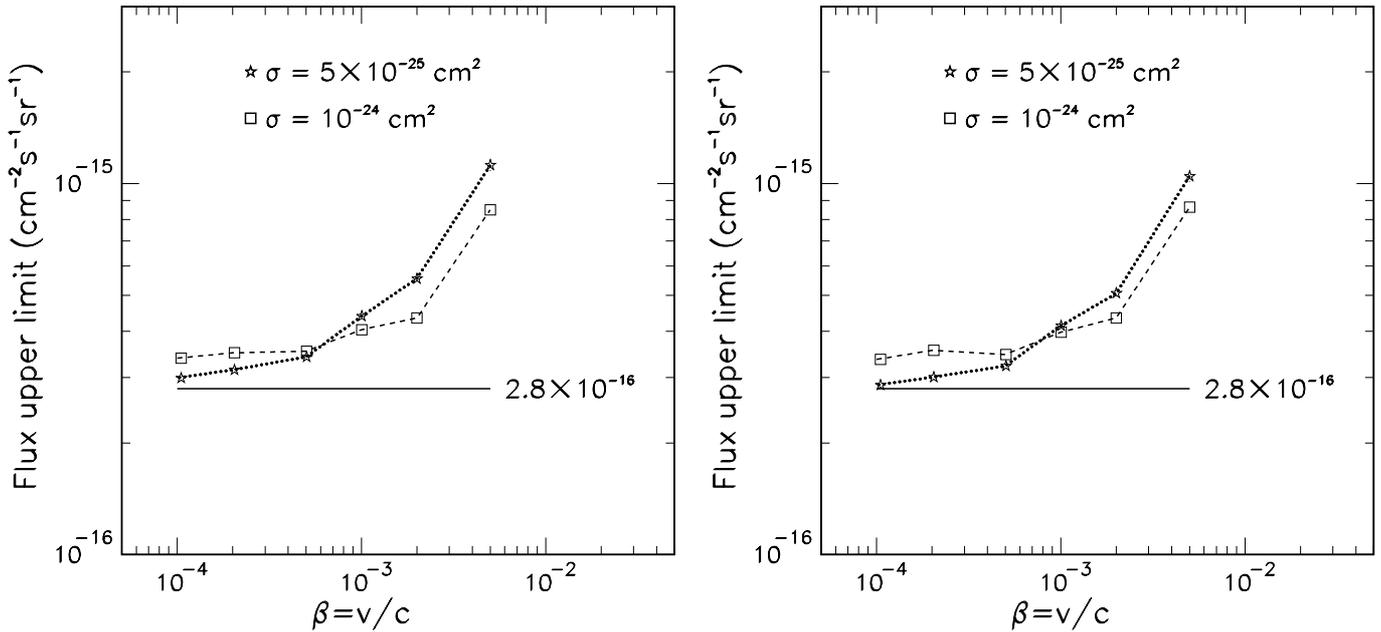
Fig. 6. Upper limits to the MM flux as a function of the MM velocity for two values of the catalysis cross section; in the left panel the proton and the neutron catalysis cross sections are equal, while in the right panel the proton cross section is enhanced by $1/\beta$, see text. (The solid line is the standard limit for MM without catalysis, using the streamer tube)

velocity increases. This trend clearly reflects the analysis efficiency behaviour. Moreover there is quite no difference between the two theoretical models on the proton cross section form.

From Fig. 7 we see that the upper limits are very stringent for higher cross sections, while for lower values, $\sigma_{cat} \lesssim 10^{-25}\ cm^2$ they are not very significant. This holds for all MM velocities.

In Table 2 the results obtained by some experiments searching for MM induced nucleon decay are summarized, together with the MACRO upper limit. It should be noted that, except partly for Soudan1, the limits obtained in this way rely on the catalysis process, so bounds to the MM flux set by these experiments depend on the catalysis cross section: if the catalysis process does not take place there are no limits at all. Moreover the underwater

Table 2. Magnetic monopole flux limits (in $cm^{-2}s^{-1}sr^{-1}$) obtained by experiments searching for nucleon decays catalyzed by a GUT MM

Experiment	Technique	Flux limit	β range
Soudan1 [10]	Proportional tubes	$8.8 \cdot 10^{-14}$	$10^{-2} \div 1$
IMB [11]	Water Cherenkov	$1 \div 3 \cdot 10^{-15}$	$10^{-5} \div 10^{-1}$
Kamiokande [12]	Water Cherenkov	$2.5 \cdot 10^{-15}$	$5 \cdot 10^{-5} \div 10^{-3}$
Baikal [13]	Underwater detector	$6 \cdot 10^{-17}$	$\simeq 10^{-5}$
MACRO	Streamer tubes	$3 \cdot 10^{-16}$	$1.1 \cdot 10^{-4} \div 5 \cdot 10^{-3}$
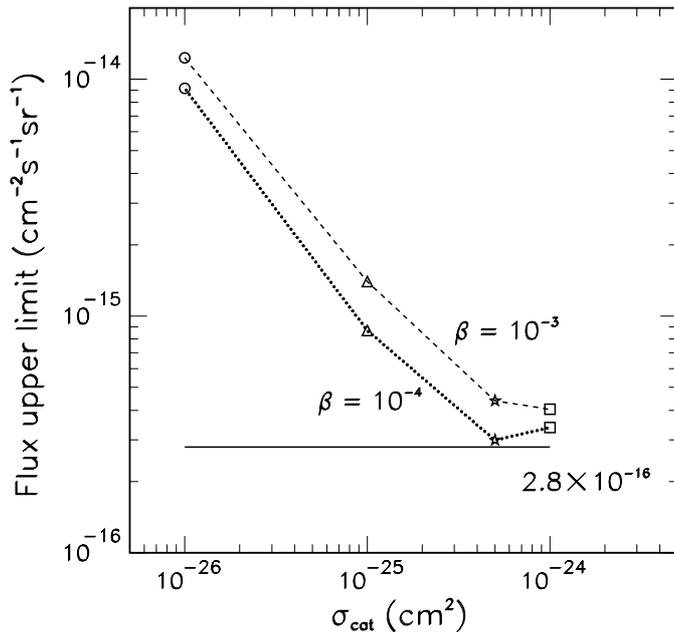
Fig. 7. Upper limits to the MM flux as a function of the catalysis cross section for two different MM velocities, as determined by this analysis

Fig. 8. Relative efficiency of the standard direct analysis applied to the simulated samples with catalysis (using the model with equal cross sections) with respect to the simulated sample without catalysis

and Cherenkov detectors must assume a very high catalysis cross section to attain the significant upper limits they quote. On the other hand MACRO can set significant limits to the MM flux, at the same level or even better than those experiments, with fewer assumptions, and its limits stand more or less the same even if the catalysis process does not take place or has a negligible cross section. In comparison with other experiments MACRO is very sensitive to small cross sections and can give good upper limits even in the presence of higher values of σ_{cat}.

Indirect bounds to the MM flux can be set also by measuring the energy emission from astrophysical objects like neutron stars and white dwarfs, which could capture and accumulate MMs in their interior: these MMs could then catalyze the decay of the nuclear matter inside them. The best limit is obtained from the measure of the diffuse X-ray background, which essentially the oldest neutron stars contribute to, and which is of the order of 10^{-23} $cm^{-2}sr^{-1}s^{-1}$ [14] (for $\beta = 10^{-3}$ and $\sigma = 10^{-25}$ cm^2); limits can be derived from the emission of single massive objects, such as the white dwarf WD 1136-286,

at the level of 10^{-20} $cm^{-2}sr^{-1}s^{-1}$ [15](again for $\beta = 10^{-3}$ and $\sigma = 10^{-25}$ cm^2). Although very impressive, nevertheless these limits are indirect and very model–dependent, especially for what concerns the estimate of the density of old neutron stars, based on the assumed birth rate, the not well known X-ray absorption in the interstellar medium, and the uncertainties in the source distance measurements. There could be also physical loopholes to the validity of these limits [14]. Of course if the MMs cannot catalyze the nucleon decay there are no bounds at all.

7 Effects of the catalysis on the standard streamer tube analysis

The standard streamer tube data analysis (along with the related hardware) is described in detail in [19]. Briefly it is based on the search for single tracks in space and time, with at least 7 points in the wire and time views and at least 6 points in the strip view; all good tracks
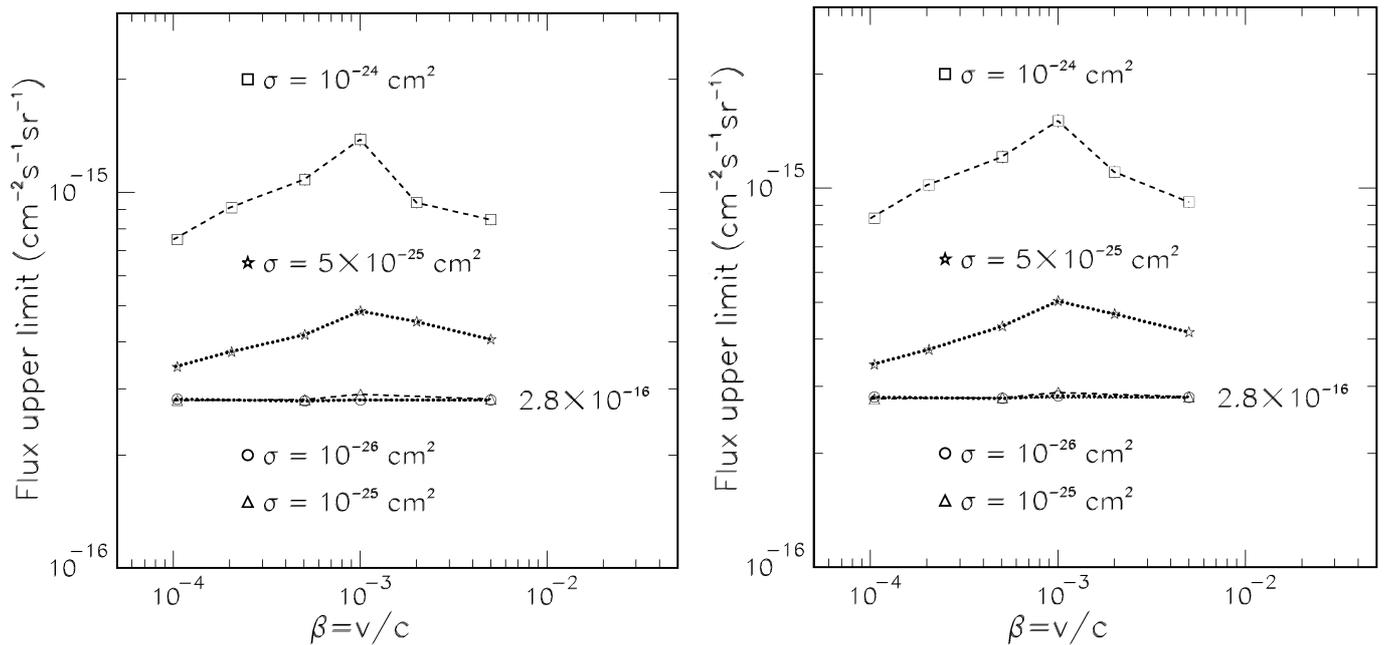
Fig. 9. Upper limits to the MM flux as a function of the MM velocity for various catalysis cross section, as determined by the standard analysis taking into account also the catalysis process, assuming the two theoretical models for the cross section form, equal for proton and neutron (left) or proton enhanced (right)

are required to have $|\beta| \leq 5 \cdot 10^{-3}$. As in the catalysis search, only the horizontal streamer planes of the lower MACRO participated in the trigger formation, both lower and upper streamer planes were used for the event reconstruction.

The standard MM search with the streamer tubes assumes that the MM does not induce the nucleon decay, hence its validity for $\sigma_{cat} \lesssim 10^{-27}$ cm^2 = 1 mb. To study the dependence of this analysis on the catalysis cross section, all the simulated samples with catalysis were analyzed with exactly the same programs used for the real data, applying all but the cut on β, and the results were compared with the simulated sample without catalysis. In Fig. 8 the ratio of the analysis efficiency for the samples with a given cross section with respect to the analysis efficiency for the sample with $\sigma_{cat} = 0$ is plotted. The behaviour of this ratio as a function of the total cross section is clear: for $\sigma_{cat} = 10^{-26}$ $cm^2 = 10$ mb the analysis efficiency is actually unchanged with respect to the case of no catalysis; also for $\sigma_{cat} = 10^{-25}$ $cm^2 = 100$ mb the efficiency is quite the same. So in both cases the catalysis does not decrease the MACRO capabilities of detecting a MM, and can even help its detection, since there is an increase in the number of triggering events (Fig. 1). Instead for $\sigma_{cat} = 10^{-24}$ $cm^2 = 1000$ mb the events are so complex and rich of hits that the standard analysis does not succeed in reconstructing most of them. This is due to the fact that at this level there are so many catalysis hits that the reconstruction procedure may fail. We think that 1000 mb is the maximum value worth to be considered, any simulation for higher values being meaningless. From this point of view $\sigma_{cat} = 5 \cdot 10^{-25}$ $cm^2 = 500$ mb can be considered an intermediate case: the typical event

is enough complicated to put in trouble the reconstruction code, but not so much as to defeat it completely.

In addition, the behaviour of the analysis efficiency as a function of the MM β is interesting: in all samples this efficiency is minimum for intermediate velocities, particularly for $\beta = 10^{-3}$. At low velocities the time track is very inclined, since the MM ToF is large, so the fit procedure can more easily distinguish it among the catalysis hits. At high velocities the fit may mix the MM hits and the catalysis hits, but since the time track is near vertical this does not imply a significant error in the ToF reconstruction. Instead, at intermediate velocities this hit mixing is very deleterious leading often to a wrong ToF estimation. In this regime in fact many of the rejected events have a reconstructed β much greater than the actual one, often near to that of a relativistic particle. Clearly, this effect is more evident for higher σ_{cat} values.

Since the data set is exactly the same as the one used in the standard published analysis, we can use the same acceptance and live time, while the analysis efficiency must be corrected for the catalysis effects. In Fig. 9 we show the new upper limits to the MM flux as obtained with the standard analysis taking into account the catalysis process as well (the quoted number is the published limit neglecting this process). For $\sigma_{cat} = 5 \cdot 10^{-25}$ cm^2 the new bounds are between 3.43 and $4.83 \cdot 10^{-16}$ cm^{-2} s^{-1} sr^{-1} for the model assuming the same decay cross section for proton and neutron, and between 3.42 and $5.04 \cdot 10^{-16} cm^{-2} s^{-1}$ sr^{-1} in the model with enhanced proton decay cross section.

Figure 10 shows how the MACRO upper limit to the MM flux obtained with the previously published analysis
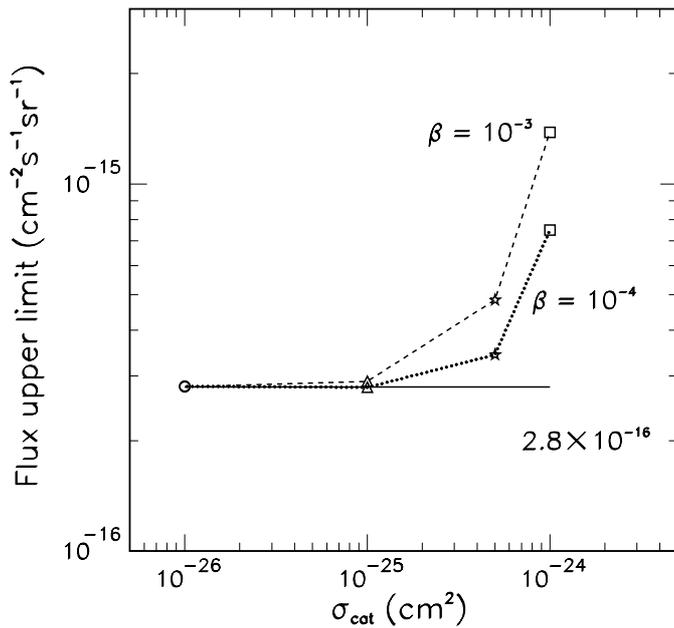
Fig. 10. Upper limits to the MM flux as a function of the catalysis cross section for two different MM velocities, as determined by the previously published direct analysis but taking into account the catalysis process as well

changes as a function of the catalysis cross section σ_{cat} for two MM velocities $\beta = 10^{-4}$ and $\beta = 10^{-3}$.

From the last Figure it can be clearly seen that the MM upper limit from the published standard streamer analysis is practically unspoiled by the catalysis process for lower cross section values. So the results of the standard streamer MM analysis, previously reported for $\sigma_{cat} < 1\ mb$ [17], can be extended to higher values of the catalysis cross section up to $\sigma_{cat} \simeq 100\ mb$. Even assuming a cross section $\sigma_{cat} \simeq 500\ mb$, the flux limit would not increase more than a factor 2.

8 Conclusions

In this paper we presented the results of a dedicated search for events of nucleon decays catalyzed by the passage of a GUT MM in the MACRO detector. The efficiency of the present catalysis–oriented analysis, which used only the streamer tube subdetector, is very good for catalysis cross sections of the order $100 \div 1000\ mb$. Since no candidate survived, a 90% C.L. upper limit to the MM flux can be set at the level of $\sim 3 \cdot 10^{-16}\ cm^{-2}\ s^{-1}\ sr^{-1}$ in the range $10^{-4} \leq \beta \leq 5 \cdot 10^{-3}$.

We have shown that a dedicated analysis based on the nucleon decay catalysis yields flux limits which are considerably more stringent than those obtained by nucleon decay experiments; we also made looser assumptions

(smaller, more reasonable cross sections, no need to have a chain of decay events to clearly identify the MM). We were able to set upper limits to the local MM flux even if the catalysis process does not take place, using a different analysis strategy; here we have shown how this previous analysis, developed in the hypothesis of no decay, depends on the catalysis cross section.

References

1. Preskill, J., Ann. Rev. Nucl. Part. Sci. **34**, 461 (1984)
2. Kolb, E.W., Turner, M.S. (1990), The Early Universe, Addison–Wesley
3. Bais, F.A. et al., Nucl. Phys. B **219**, 189 (1983)
4. Rubakov, V.A., JETP Lett. **33**, 644 (1981)
5. Rubakov, V.A., Serebryakov, M.S., Nucl. Phys. B **218**, 240 (1983)
6. Callan, C.G., Phys. Rev. D **26**, 2058 (1982)
7. Callan, C.G., Nucl. Phys. B **212**, 391 (1983)
8. Ellis, J., Nanopoulos, D.V., Olive, K.A., Phys. Lett **116B**, 127 (1982)
9. Arafune, J., Fukugita, M., Yanagita, S., Phys. Rev. D **32**, 2586 (1985)
10. Bartelt, J. et al., Phys. Rev. D **36**, 1990 (1987)
11. Becker-Szendy, R. et al., Phys. Rev. D **49**, 2169 (1994)
12. Kajita, T. et al., J. Phys. Soc. Jpn. **54**, 4065 (1985)
13. Balkanov, V.A. et al., Prog. Part. Nucl. Phys. **40**, 391 (1998)
14. Kolb, E.W., Turner, M.S., Ap. J. **286**, 702 (1984)
15. Freese, K., Krasteva, E., (1999) Phys. Rev. D **59**, 063007
16. Turner, M.S., Parker, E.N., Bogdan, T.J., Phys. Rev. D **26**, 1296 (1982)
17. Ambrosio, M. et al. Final results of magnetic monopole searches with the MACRO experiment hep-ex 0207020
18. Ahlen, S.P. et al., Phys. Rev. Lett **72**, 608 (1994)
19. Ambrosio, M. et al., Astrop. Phys. **4**, 33 (1995) and References therein
20. Ambrosio, M. et al., Phys. Lett B **406**, 249 (1997)
21. Ambrosio, M. et al., Astrop. Phys. **6**, 113 (1997)
22. Ambrosio, M. et al. (2001), hep-ex/0110083, accepted by Astrop. Phys.
23. Ahlen, S.P. et al., Nucl. Inst. Meth. A **324**, 337 (1993)
24. Ambrosio, M. et al., Nucl. Inst. Meth. A **486**, 663 (1993)
25. Drell, S.D. et al., Phys. Rev. Lett **50**, 644 (1983)
26. Patera, V., Phys. Lett A **137**, 259 (1989)
27. De Mitri, I. et al., Nucl. Inst. Meth. A **360**, 311 (1995)